ELSEVIER

Journal of Power Sources 81–82 (1999) 8–12

JOURNAL OF POWER SOURCES

www.elsevier.com/locate/jpowsour

Characterisation of the ambient and elevated temperature performance of a graphite electrode

Anna M. Andersson, Kristina Edström, John O. Thomas *

Inorganic Chemistry, Ångström Laboratory, Uppsala University, Box 538, SE-751 21 Uppsala, Sweden

Abstract

Thermal stability of the SEI layer on graphite in < Li|liquid electrolyte|graphite > half-cells has been investigated. DSC measurements reveal a two-stage exothermal reaction. The first, corresponding to a breakdown of the SEI layer, begins at 58°C for a 1 M $LiBF_4$ in EC/DMC 2:1 electrolyte. The second, starting at ~80°C, corresponds to lithium deintercalation, followed by some irreversible chemical reaction; the heat evolved in the second stage increases for increasing lithium content in the graphite. Precycling at RT to generate the Solid Electrolyte Interface (SEI) layer, followed by storage for 1 week at different temperatures and then continued cycling, brings about a rapid decline in capacity for cells stored above 50°C. XRD could also show that graphite electrodes are partially blocked for subsequent lithium-ion insertion after such treatment. ESCA (XPS) characterisation of the surface of fresh graphite electrodes compared with that of graphite electrodes extracted from these RT precycled/stored cells gives evidence of the formation of a thicker macroscopic layer on the electrode surface of cells stored at 60°C. This layer is *not* found for half-cells stored at lower temperatures.

Keywords: Li-ion battery; Graphite electrode; Lithium intercalation; Thermal stability; SEI layer

1. Introduction

It is by now well established that there are corrosion and safety problems associated with the 'rocking-chair' $C/LiMn_2O_4$ Li-ion battery concept [1–4]. Poor electrochemical performance has been encountered above 55°C. There is a general feeling that this is due largely to the instability of the $LiMn_2O_4$ phase; Mn^{2+}-ion dissolution into the liquid electrolyte has been found to be dependent on temperature, cathode potential and type of electrolyte. The dissolved Mn^{2+} ions have been located not only in the electrolyte but also on the surface of the anode [1–4].

However, this may not be the whole story: the *anode* of a 'rocking-chair' Li-ion battery is nowadays often a graphitic material with Li^+ ions intercalating into the graphite structure on charging. Moreover, an irreversible capacity loss also occurs during the first charge/discharge cycle, corresponding to the formation of a thin solid–electrolyte-interface (SEI) layer on the surface of the graphite grains [5–8]. Since lithium/graphite intercalation compounds, LiC_x, are thermodynamically unstable in all known electrolytes, the function of this SEI layer is to protect the graphite grains from cointercalation of solvent molecules between the graphene planes, while still permitting the transport of lithium ions. The electrolytes most commonly used today which can provide this protective SEI-layer are solutions of EC (ethylene carbonate) and DMC (dimethyl carbonate) or DEC (diethyl carbonate) and some lithium salt.

The question thus arises as to whether the instability of this SEI layer plays an important (not to say decisive) role in the capacity-loss mechanism at elevated temperatures. We focus here on the behaviour of graphite electrodes in 'half-cells', where the counter electrode is a lithium-foil. In this way, we are able to isolate the influence of temperature on the SEI layer from the effects of Mn-corrosion. In this connection, we have also chosen to use $LiBF_4$ as salt, dissolved in EC/DMC, since it is known to cause lower leakage of manganese ions into the electrolyte than other electrolyte salts in the complete < C|liquid electrolyte|$LiMn_2O_4$| > cell [9]. It is of interest to probe whether $LiBF_4$ performs as well on the low voltage side as it does on the high-voltage (cathode) side of the battery.

A combination of thermal analysis (DSC), electrochemical cycling, XRD and ESCA surface analysis have, there-

* Corresponding author. E-mail: josh.thomas@kemi.uu.se

0378-7753/99/$ - see front matter
PII: S0378-7753(99)00185-8

fore, been used here to probe the thermal stability of the graphite anode in a lithium-ion battery context.

2. Electrode preparation

After a series of optimisation experiments, all electrodes used in this study were prepared by spreading a mix of 90 wt.% Timrex KS6 (Timcal A + G, Sins, Switzerland), 5 wt.% Shawinigan Black (SB) carbon powder and 5 wt.% EPDM rubber binder in cyclohexane onto a porous 25-μm thick Ni-foil current collector. The graphite loading on the current collector was 5.4 mg/cm^2. The electrodes were then dried at 120°C for a few hours, cut into 3.1 or 7.0 cm^2 pieces, again dried overnight under vacuum at 120°C, before laminating them in an Ar-filled glovebox (< 1 ppm H_2O and O_2) against a glass-wool separator soaked in electrolyte and pressed onto a lithium-foil counter electrode. The laminates were packed in polymer coated aluminium bags, evacuated and sealed. The electrolyte used was 1 M $LiBF_4$ (Tomoyama) in EC/DMC 2:1 (Selectipur®, Merck, Darmstadt, Germany).

3. DSC measurements

All DSC measurements were conducted using a Mettler TA 4000 system. The various components of the half-cells were studied separately and in all possible combinations: Li(s), Li(s) + electrolyte, graphite, nickel-foil, EC, DMC, EPDM, $LiBF_4$, EC + DMC 2:1, EC + DMC 2:1 + $LiBF_4$, and all possible combinations thereof. This was done in the temperature range −150°C to 300°C at a 5°/min rate.

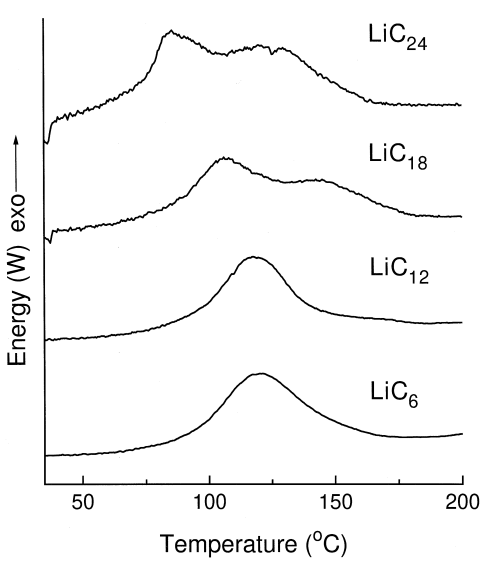

Fig. 1. DSC curves for the different lithium intercalated graphite phases, LiC_{24}, LiC_{18}, LiC_{12} and LiC_6. Note: the curves are plotted on different arbitrary scales; see Table 1 for some indication of the relative scales.

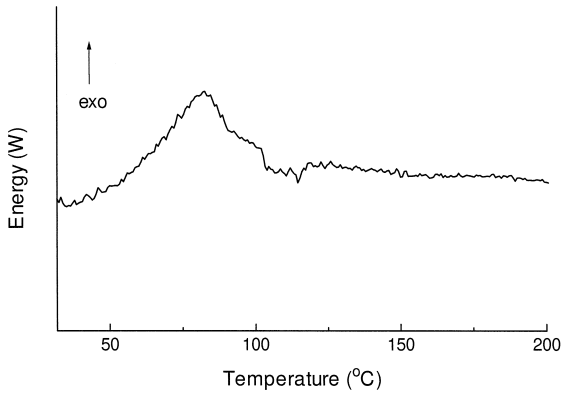

Fig. 2. A DSC curve for a deintercalated graphite anode ($x = 0$) that has been through a discharge/charge cycle. Vertical axis has the same scale as for the $x = 24$ case in Fig. 1.

Finally, the various intercalation stages of graphite were studied (LiC_6, LiC_{12}, LiC_{18} and LiC_{24}), as extracted from half-cells. All 'coffee-bag' type half-cells were dismantled under argon in the glovebox, and the electrodes (coated with a thin layer of electrolyte) were cut into standard round samples which were then sealed into standard Al crucibles. The Ni-foil substrate was placed against the Al surface to ensure a minimum of contact between the walls of the crucible and the LiC_x samples. The same amount of Ni-foil was used as reference in a standard Al crucible. A typical sample weight was 5 mg. The LiC_x samples were measured in the temperature range 30–300°C.

None of the various combinations of materials measured in this way showed evidence of any reaction in the range 30–200°C. The electrolyte ($LiBF_4$ + EC/DMC) boils at ~250°C, and pure lithium foil melts at ~190°C.

The LiC_x runs show a two-step exothermal reaction; the first beginning at 58°C and the second at ~80°C (Fig. 1). A deintercalated graphite electrode was also measured after one discharge/charge cycle to form the SEI layer (Fig. 2). Only the first step is observed for the deintercalated graphite; suggesting strongly that it is associated with the breakdown of this SEI layer. The heat evolved during this first step is approximately the same for all LiC_x samples (Fig. 1) while, for the second step, it increases with increasing lithium content (Table 1). This reaction must, therefore, be associated with lithium-ion depletion of

Table 1
Total heat evolved for lithium intercalated graphites and a deintercalated electrode using a 1 M $LiBF_4$ in EC/DMC 2:1 electrolyte in the temperature range 50–180°C

LiC_x compound	ΔH [J/g]
Deintercalated electrode	33
LiC_{24}	120
LiC_{18}	171
LiC_{12}	234
LiC_6	315

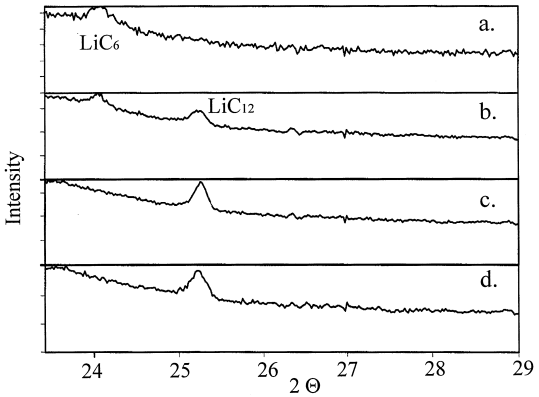

Fig. 3. In situ X-ray diffractograms (CuKα_1 radiation) for a fully intercalated LiC_6 cell stored for 1 week at 60°C; (a) after 1 h, (b) after 4 h, (c) after 12 h and (d) after 1 week.

the graphite host. Cooling heat-treated intercalated graphites from 300°C to room temperature showed that the reaction is irreversible, and a subsequent heating of the same sample showed no such reaction.

4. Electrochemical cycling and in situ XRD

In situ XRD studies were made using a purpose built heating attachment for a STOE & CIE powder diffractometer fitted with a position-sensitive wire detector. The device facilitates oscillation of the cell (in its own plane)

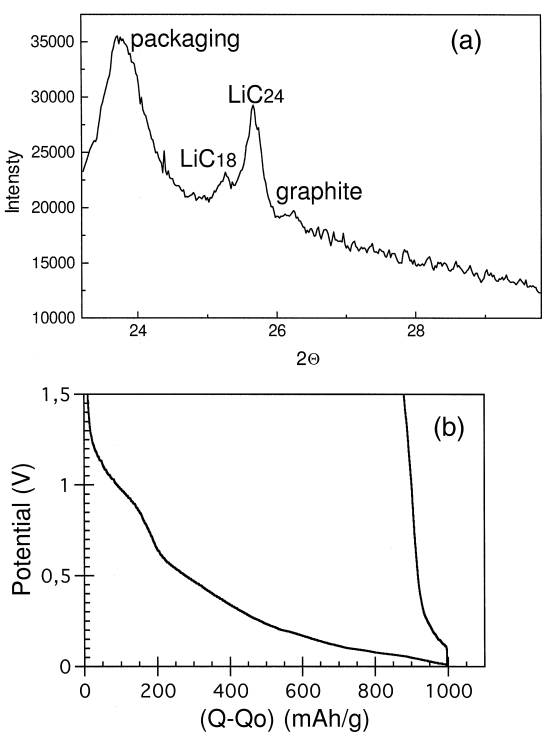

Fig. 4. In situ X-ray diffractogram for a half-cell at 0 V after cycling at 80°C (a), and the corresponding first (and only) discharge/charge curve (b).

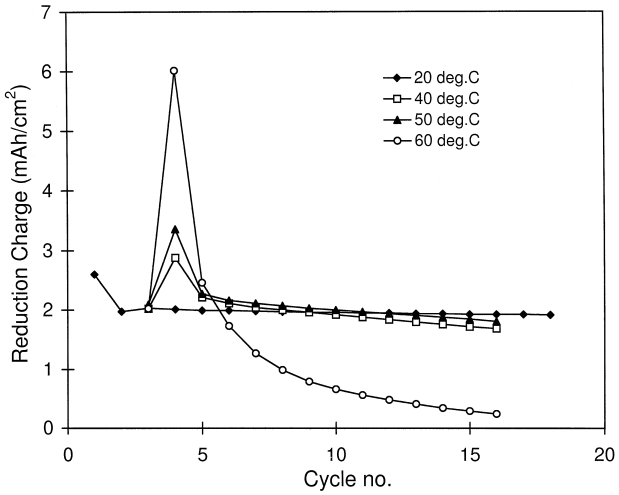

Fig. 5. Reduction charge vs. cycle number for Li/graphite half-cells precycled three times at room temperature (cycle nos. 1–3) prior to storage at different temperatures for 7 days, followed by continued cycling at these same temperatures.

through 180° to provide a more representative diffraction average [10]. A fully intercalated LiC_6 electrode was prepared at room temperature, heated to 60°C, and then stored for 1 week at this same temperature while its (001) peak was monitored. A phase transformation from LiC_6 to LiC_{12} occurred after less than 10 h; no further phase changes was observed during the duration of the experiment (Fig. 3).

Galvanostatic cycling of half-cells at 80°C failed on the first discharge/charge cycle. In situ diffraction showed that it was not possible to achieve more than a LiC_{18} compound (Fig. 4a); the corresponding cycling curve showed a high irreversible capacity loss (Fig. 4b), suggesting the formation of a macroscopic scale SEI layer.

Electrochemical cycling at room temperature followed by storage at different temperatures for 7 days resulted in a clear decline in cell capacity between 50 and 60°C on continued cycling (Fig. 5).

5. ESCA measurements

The ESCA measurements were conducted on a PHI 5500 system, using a AlKα excitation source. Cells subjected to the various pre-treatments were dismantled in the glovebox, and small pieces of the graphite electrodes were mounted on the XPS sample holder. These were then vacuum-sealed in a polymer laminated aluminium bag in the glovebox, and transported to the ESCA apparatus, where they were removed and placed in the spectrometer introduction chamber under a flow of dry N_2(g). The samples were first analysed as prepared, and then sputtered with an Ar beam and analysed intermittently until the amounts of the various elements reached a steady state.

The elements found on the surface of the graphite electrode were, in all cases: F, O, C, B and Li, where

certain peak shifts could be assigned directly to the $LiBF_4$ salt, LiF and graphite. The amount of each element was calculated by integrating the intensities of the ESCA peaks and correcting for the ionisation cross-section of each element. Since the samples had not been washed, the contributions from $LiBF_4$ and graphite were subtracted in the elemental analysis of the surface layer. The concentrations of the various elements found on the surface of the stored and unstored samples are given in Fig. 6. An increase in Li and F content occurs on storage at RT and 40°C. The shifts in the Li and F peaks were assigned to the formation of LiF.

The C and O content on the surface increased significantly for the sample stored at 60°C (Fig. 6a). The C and O increase is coupled to a decrease in Li and F content. Fig. 6b shows the molar ratios of the elements on the graphite surface after Ar sputtering. When the outer layer of the electrode had been removed, it is clear that the electrodes had a very similar composition. However, while a compositional 'steady state' was reached for the samples stored at RT and 40°C after less than 40 s, a constant 'pure graphite' concentration was not observed until after more than 10 min for the electrodes stored at 60°C.

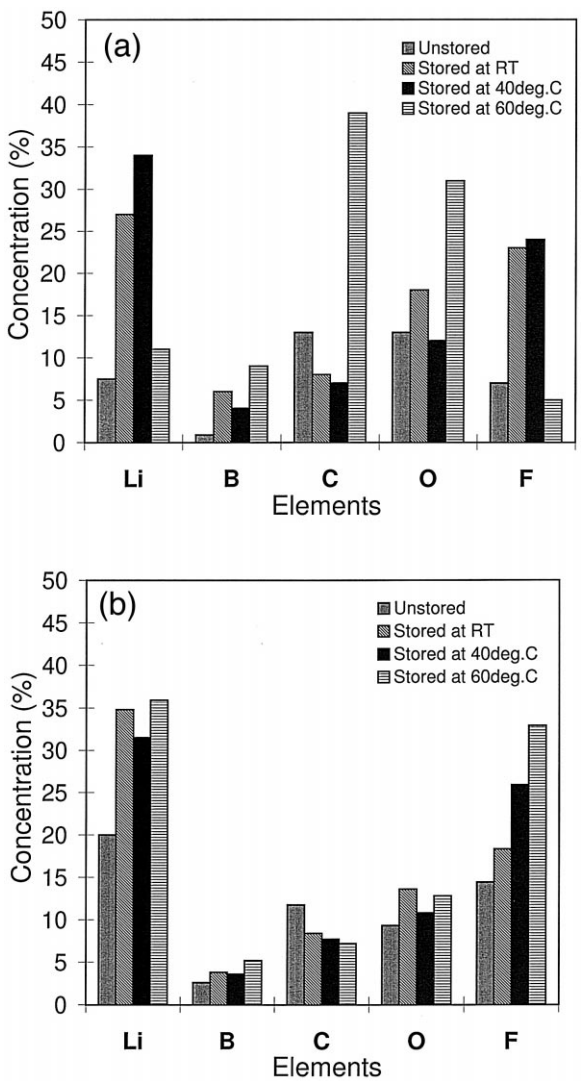

Fig. 6. ESCA analysis of the SEI layers formed at different temperatures (a), and of the SEI-layers remaining after argon sputtering (b).

6. Discussion

The results derived above combine to provide a more complete picture of the factors influencing the original thermal stability of the SEI layer on graphite.

The exothermal reaction in deintercalated and intercalated LiC_x samples, which begins at 58°C for the $LiBF_4$ salt case, can be assigned to the breakdown of the SEI-layer. This is a significantly lower temperature than for the same type of solvent containing other lithium salts, e.g., ~104°C $LiCF_3SO_3$ [4], and ~105°C for $LiPF_6$ [11]. The second stage of the exothermal reaction, which involves the depletion of lithium from the graphite electrode followed by other chemical reactions, also begins at a lower temperature (~80°C) for the $LiBF_4$ case than for electrolytes containing other salts [11]. Note that a first-order melting transition has been observed at 715 K in chemically intercalated LiC_6 [12,13] which is considerably higher than that measured here. It would seem that a chemical reaction begins above 50°C which involves lithium ions and the electrolyte or the electrolyte degradation products. An additional thicker SEI layer appears in the charged state on top of the original SEI layer; this second layer covers the entire graphite electrode surface, and results in delithiation of the electrode [1,6,11]. A more detailed analysis of the reactions taking place here is underway.

Electrochemical cycling of half-cells after storage at different elevated temperatures indicates a partial blocking of the graphite electrode surface to lithium intercalation. The fully intercalated state, LiC_6, is never again attained after storage at 60°C, as shown by in situ XRD (Fig. 4a).

ESCA analysis also gives evidence of this same type of blocking mechanism for graphite electrodes cycled at room temperature and then stored for 7 days above 50°C. In addition to the initially formed thin SEI layer, ESCA can confirm the formation of this macroscopic layer which coats the entire electrode surface. This layer could be removed by Ar sputtering to reveal the same type of thin SEI layer also formed on each graphite particle at lower temperatures. Note that this thicker layer is *not* generated on graphite anodes stored for 7 days at 50°C and lower. Finally, it should also be borne in mind that there are many other parameters, e.g., type of carbon used, electrode morphology (particle size, shape and orientation), choice of binder, etc., which will also influence the formation and thermal stability of the SEI layer. The major result of this present study is that the *composition of the electrolyte* used has a decisive influence.

7. Conclusions

The thermal stability of the SEI layer on a graphite surface using $LiBF_4$ in EC/DMC 2:1 is shown here to be a real safety risk. Of the various lithium salts studied, $LiBF_4$ is found to produce the SEI layer with the lowest decomposition temperature.

It is clear, therefore, that metal-ion dissolution of the cathode is not the only factor responsible for poor electrochemical performance at elevated temperatures; chemical reactions on the anode side can be equally (not to say more) critical. Irreversible reactions involving the SEI layer can begin below 60°C at the surface of graphite anodes. More detailed studies are underway to better understand the complexities of SEI-layer formation and breakdown on a graphite electrode.

Acknowledgements

This work has been supported by the EU (Joule III) Programme, and in Sweden by The Swedish Natural Science Research Council (NFR), The Board for Technical Development (NUTEK), and The Foundation for Environmental Strategic Research (MISTRA). The authors would like to thank Dr. Åsa Wendsjö and Dr. Ningling Rao Danionics, Odense, Denmark and Mr. Torvald Andersson, Uppsala University, for their support and interest in this work.

References

[1] A. Blyr, C. Sigala, G. Amatucci, D. Guyomard, Y. Chabre, J.-M. Tarascon, J. Electrochem. Soc. 145 (1998) 194.
[2] G. Amatucci, A. Blyr, C. Sigala, P. Alfonse, J.-M. Tarascon, Solid State Ionics 104 (1997) 13.
[3] G. Amatucci, C.N. Schmutz, A. Blyr, C. Sigala, A.S. Gozdz, D. Larcher, J.-M. Tarascon, J. Power Sources 69 (1997) 11.
[4] D.H. Jang, Y.J. Shin, S.M. Oh, J. Electrochem. Soc. 143 (1996) 2204.
[5] M. Jean, A. Tranchant, R. Messina, J. Electrochem. Soc. 143 (1996) 391.
[6] D. Aurbach, Y. Ein-Eli, B. Markovsky, A. Zaban, S. Luski, Y. Carmeli, H. Yamin, J. Electrochem. Soc. 142 (1995) 2882.
[7] E. Peled, D. Golodnitsky, G. Ardel, V. Eshkenazy, Electrochim. Acta 40 (1995) 2204.
[8] U. von Sacken, E. Nodwell, A. Sundher, J.R. Dahn, J. Power Sources 54 (1995) 240.
[9] D.H. Jang, S.M. Oh, J. Electrochem Soc. 144 (1997) 3342.
[10] T. Eriksson, A.M. Andersson, Ö. Bergström, H. Björk, T. Gustafsson, J.O. Thomas, in manuscript.
[11] A. Du Pasquier, F. Disma, T. Bowmer, A.S. Gozdz, G. Amatucci, J.-M. Tarascon, J. Electrochem. Soc. 145 (1998) 472.
[12] J. Rossat-Mignod, A. Wiedenmann, K.C. Woo, J.W. Milliken, J.E. Fischer, Solid State Commun. 44 (1982) 1339.
[13] V.V. Avdeev, A.P. Savchenkova, L.A. Monyakina, I.V. Nikolskaya, A.V. Khvostov, J. Phys. Chem. Solids 57 (1996) 947.